Depressions at the surface of an elastic spherical shell submitted to external pressure

C. Quilliet
Laboratoire de Spectrométrie Physique, CNRS UMR 5588 & Université Joseph Fourier, 140 avenue de la Physique, 38402 Saint-Martin d'Hères Cedex, France
and Soft Condensed Matter, Debye Institute, Utrecht University, Princetonplein 5, 3584 CC Utrecht, The Netherlands
(Received 21 March 2006; published 13 October 2006)

Elasticity theory calculations predict the number N of depressions that appear at the surface of a spherical thin shell submitted to an external isotropic pressure. Using a model that mainly considers curvature deformations, we show that N depends on the relative volume variation and on an adimensional parameter that takes into account both the relative spontaneous curvature and the relative thickness of the shell. Equilibrium configurations show single depression ($N=1$) for small volume variations, then N increases, at maximum up to 6, before decreasing more abruptly due to steric constraints, down to $N=1$ again for maximal volume variations. These static predictions are consistent with previously published experimental observations.

DOI: 10.1103/PhysRevE.74.046608 PACS number(s): 46.70.De, 46.32.+x, 89.75.Kd

I. INTRODUCTION

Buckling, or sudden change of the shape of objects under constraint, has been a problem addressed for a long time, as it is of utmost practical importance (architecture, designing of tough containers or pipes) [1–3]. More recently, buckling was investigated at much smaller scales, mainly due to the improvement of observation and manipulation techniques at microscopic, or even nanoscopic level [4]. This brings back into the spotlight the simplest symmetry that provides a closed vessel, the spherical one. In spite of important theoretical advances motivated by air and spatial navigation [5], the spherical symmetry had been somewhat neglected compared to other symmetries (axisymmetrical, cylindrical, etc.) because it is less directly encountered in large scale systems where gravity plays a role. At smaller scales, when gravity becomes negligible, whole spheres are more commonplace: they are encountered in colloids, biological objects, and in most of the phenomena linked to surface tension. Flows, encapsulations processes and evaporation/dissolution phenomena in complex fluids may lead to buckling processes, generating nontrivial shapes. Motivated by recent experimental works [6–8], we focus in this paper on thin spherical shells of an elastic and homogeneous material submitted to an isotropic constraint, such as an external pressure. The onset of buckling of hollow spheres submitted to an external pressure has been derived in earlier times [9,10], recent theoretical work deals mainly with the nonideality of materials [11]. For what concerns postbuckling, no analytical predictions concerning postbuckling shapes of spheres under isotropic external pressure are available, by lack of a complete buckling analysis.

Indeed, there is a lively field in biophysics aimed at understanding shapes of biological objects with simple physical ingredients. Since early work by Helfrich [12] and others where bending elasticity and spontaneous curvature (or area-difference elasticity [13], which can be modeled in the same way [14]) were the main shape tuners [15], some models now include additional stretching elasticity, which brings them quite close to what is discussed here. To our knowledge, they are nevertheless inaccurate to interprete the buckling of homogeneous shells, as they precisely take into account inhomogeneities characteristic of the biological objects they aim to describe: e.g., either the different origin (lipidic membrane and cytoskeleton) of bending and stretching elasticity [14,16], which allows relative values forbidden in a model of thin homogeneous plate, or defects due to the discrete protein structure of a shell virus [17].

In this paper concerning homogeneous objects, we propose a heuristic calculation concerning the optimum number of depressions that can be held by a buckled, thin, spherical shell in order to understand the apparently divergent observations of Refs. [6] and [7]. These two papers reported the observation of strongly buckled objects, originally porous hollow spherical shells filled with a solvent, that buckle when the solvent evaporates. Buckling of a porous shell due to evaporation of an inner solvent is acknowledged as being of a capillary origin, and macroscopically (i.e., at scales larger than the pore size) equivalent to the effect of an isotropic external pressure [18]. These experiments therefore constitute a direct illustration of the postbuckling of hollow spheres under external pressure, for which no theoretical predictions exist. Surprisingly, conformations taken by the shells qualitatively differ between Refs. [6] and [7]. As shown in Fig. 1(a), there is occurrence of either a single and quite deep depression [6], or several depressions distributed over the sphere's surface, leading to a coarsely cubic shape [7]. Single depression was also obtained by osmotic pressure (Fig. 1(b) and [8]). In this paper we will determine whether this discrepancy can be interpreted through the equilibrium configurations of an elastic model, or if some drying artifacts should be invoked.

II. ELASTICITY

We will use elasticity theory results related to thin shells submitted to external constraints in order to get insight into the number of depressions expected for an equilibrium conformation. For a thin, spherical shell of homogeneous elastic material (Young's modulus E_{3D}, sphere radius R, thickness d), deformation occurs by bidimensional stretching (stretch modulus $E_{2D}=E_{3D}d$) or bending (bending modulus

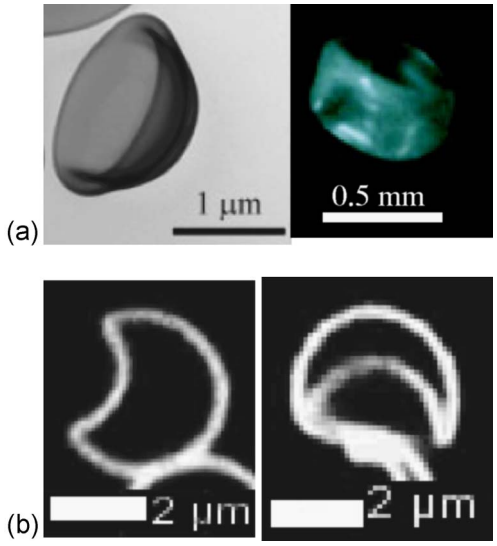

FIG. 1. (Color online) Different shapes obtained after evaporation of the solvent contained in a spherical porous shell. (a) Left: Silica/silicon ≪capsule≫ ($N=1$; $d/R=0.17$) observed by Zoldesi *et al.* [6] (reproduced with author and editor permission). Right: More polyhedral shape ($N\sim 6$) observed by Tsapis *et al.* in shells made from aggregation of colloidal particles at the surface of an evaporating droplet of colloidal suspension [7]; $d/R=0.09$ (reproduced with permission by the author). (b) Deformation of polyelectrolyte capsules ($d/R=0.026$) in solution through osmotic pressure (left: 22 kPa; right: 44.5 kPa) [8].

$\kappa\sim E_{3D}d^3$). The latter is related to the mean curvature, and we do not take into account energy variations linked to the Gaussian curvature, as its integral on a closed surface depends only on the topology (Gauss-Bonnet theorem). It has been shown [9] that the ratio between bending and bidimensional stretch energies scales as

$$U_b/U_s \sim (d/R)^2,$$

where R is the radius of the spherical shell and d its thickness. Hence, for sufficiently thin shells, deformations occur mainly by bending, which is much less energetic than stretching. In this framework, a depression obviously corresponds to the inversion of a spherical cap [9,10], which avoids stretching energy outside the circular ridge that joins the undeformed part and the inverted cap, defined by its half-angle α (Fig. 2). For shells of zero spontaneous curvature (the case with nonzero spontaneous curvature will be treated later), bending energy does not depend on the sign of the curvature and hence is not modified in the inverted cap. Energy modifications then concentrate in the circular ridge, having a lateral extension imposed by minimization as $\delta\sim(Rd)^{1/2}$; the relevant curvature radius is $\delta/\tan\alpha$ [10,19]. As the total surface bended in the ridge has a width δ and a length $2\pi R\sin\alpha$, the energy of a single depression writes

$$U_1 = 2\pi\kappa(d/R)^{-1/2}\sin\alpha\tan^2\alpha. \quad (1)$$

This expression diverges when α approaches $\pi/2$; thin shell theory breaks down when the radius of curvature becomes of order d. However, as will appear obvious later, other considerations different from energetic ones prevail in this limit, and looking for a more accurate expression is unnecessary within the current work.

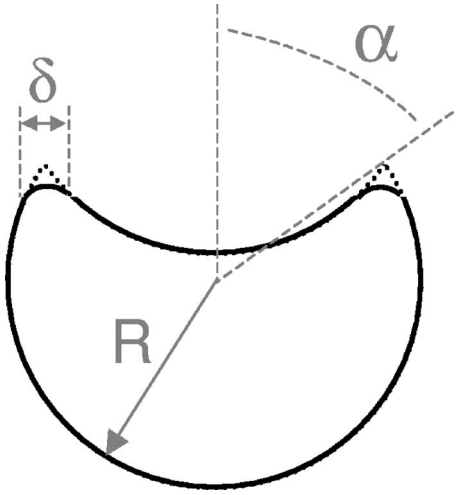

FIG. 2. Depression formed by inversion of a spherical cap. The circular ridge that allows a continuous junction between the undeformed spherical part and the inverted cap has a lateral extension $\delta\sim(Rd)^{1/2}$ (where d is the thickness of the shell). The aperture of the depression is defined by the half-angle α that extrapolates (dotted line) the ridge thickness down to zero.

The volume variation ΔV due to cap inversion is twice the volume of the spherical cap; hence, the volume variation relative to the undeformed sphere volume is

$$(\Delta V/V_{\text{sphere}})_{1\ \text{depression}} = (1-\cos\alpha)^2(2+\cos\alpha)/2. \quad (2)$$

In the case of N similar depressions, we have

$$U_N = NU_1 \quad (3a)$$

and

$$\Delta V/V_{\text{sphere}} = N(\Delta V/V_{\text{sphere}})_{1\ \text{depression}}. \quad (3b)$$

We therefore have the expressions of both the elastic energy and the volume variation corresponding to N similar depressions formed by inversion of spherical caps of half-angle α. As the relative volume variation is the key parameter to appreciate the deformation intensity, it would be interesting to eliminate α in order to get the elastic energy U_N as a function of $\Delta V/V_{\text{sphere}}$, and then to discuss the relative stability of the conformations with different numbers N of depressions ("states").

A. Explicit expression for small depressions

For small inverted caps ($\alpha\ll 1$), system (3) simplifies to

$$U_N \sim 2\pi N\kappa(d/R)^{-1/2}\alpha^3 \quad \text{and} \quad \Delta V/V_{\text{sphere}} = N\alpha^4/8,$$

which, for a given relative volume variation $\Delta V/V_{\text{sphere}}$, leads to

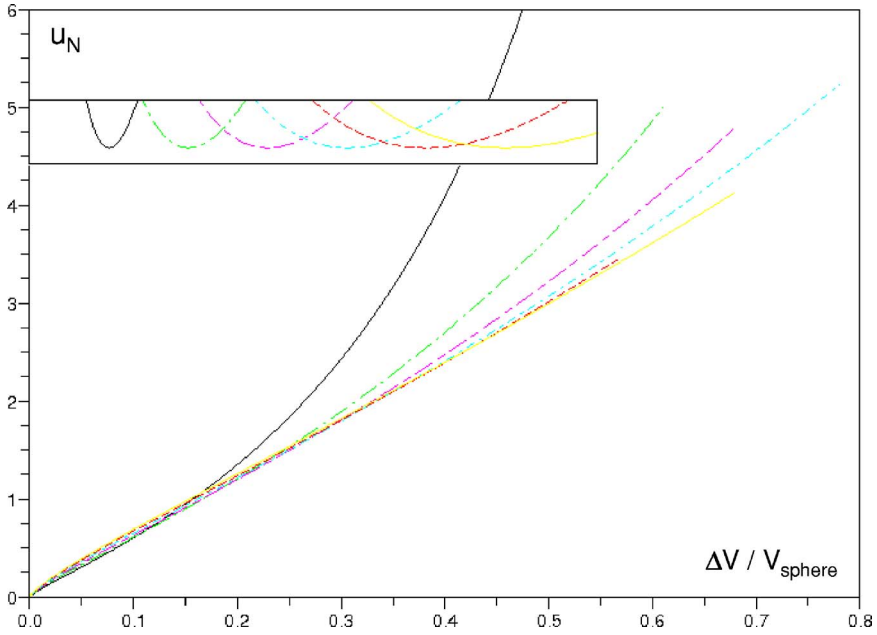

FIG. 3. (Color online) Reduced energy $u_N = U_N/[2\pi\kappa(d/R)^{-1/2}]$ as a function of $\Delta V/V_{sphere}$, for different numbers N of similar depressions (inverted spherical caps). The curves are traced up to the maximum value $(\Delta V/V_{sphere})_{max,N}$ above which there would be an interpenetration between depressions. Black (continuous line), green (long dash dot), pink (dash long dash), blue (dash dot), red (dash), and yellow (continuous) curves correspond, respectively, from $N=1$ up to 6. Note the $(\Delta V/V_{sphere})^{3/4}$ behavior of Eq. (4) for small $\Delta V/V_{sphere}$ that corresponds to small values of α. Inset: $u_N/(\Delta V/V_{sphere})$ as a function of $\Delta V/V$ (same scale in abscissa), displayed to enhance the difference between curves without modifying the $\Delta V/V$ crossover values.

$$U_N \sim 8^{13/12}\pi N^{1/4}\kappa(d/R)^{-1/2}(\Delta V/V_{sphere})^{3/4}. \quad (4)$$

For a given shell (E, d, and R fixed), the $N^{1/4}$ dependence with $\Delta V/V_{sphere}$ clearly leads to $N=1$ at equilibrium. The conformation with a single depression is favored in this regime, which corresponds to small deformations $(\Delta V/V_{sphere} \ll 1)$.

B. Implicit dependence for larger depressions

For larger values of α, a parametric plot of U_N as a function of $\Delta V/V_{sphere}$ shows that for increasing $\Delta V/V_{sphere}$, the lowest energy state changes from $N=1$ to 2 to 3, etc. (Fig. 3). However, system (3) is not sufficient to describe the conformations adopted at high deformations, since Eq. (3b) is valid only as long as depressions do not interpenetrate each other. There is, of course, a maximum size (i.e., maximum α) above which it becomes impossible to find an arrangement of N similar depressions that avoids interpenetration between two of them. For the sake of simplicity, we will neglect the thickness of the circular ridge, which corresponds to the case $d \ll R$. Then the problem becomes purely geometrical: How many similar spherical caps can be inverted without interpenetration at the surface of a sphere?

A necessary condition is that the spherical caps themselves do not overlap before inversion. This amounts to the search for the maximum surface of a sphere that can be covered with N similar spherical caps, which is another formulation of the so-called Tammes' problem: maximize the minimum point-to-point distance for a set of N points placed on a sphere [20]. The solution of the Tammes' problem is much

TABLE I. Maximum values $\alpha_{N,max}$ of the half-angle α that defines a spherical cap at the surface of a sphere, over which one cannot invert N similar caps without interpenetration. Values of α_{max} for cases $N=1-4$ are specifically treated in the text. Values for $N=5-8$ correspond to the Tammes' problem and are given in Ref. [22], $N=9$ in [27], and $N=10-15$ in [23]. For N higher than the values displayed in this table, the asymptotic formula [28] for the upper limit $\alpha_{max,N}(\text{rad}) = (2\pi/\sqrt{3})^{1/2}\ N^{-1/2}$ shows that it keeps decreasing; higher values of N are then useless for our purpose. Third column: The corresponding volume variation for the N inverted caps.

N	α_{max} (deg)	Maximum $\Delta V/V_{sphere}$
1	90	1
2	60	0.625
3	54.7	0.691
4	52.2	0.785
5	45.0	0.581
6	45.0	0.697
7	38.9	0.480
8	37.4	0.474
9	35.3	0.427
10	33.1	0.373
11	31.7	0.350
12	31.7	0.382
13	28.6	0.277
14	27.8	0.270
15	26.8	0.251

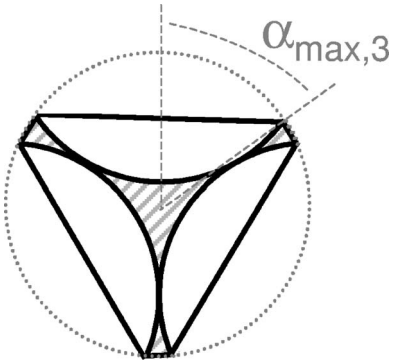

FIG. 4. Equatorial section of the $N=3$ conformation: $\alpha_{\max,3}=54.74°$. The solution to Tammes' problem would correspond to slightly larger spherical caps ($\alpha=60°$) that could not revert without interpenetration.

less obvious than its formulation. Depending on N, analytical or numerical solutions exist [21–23] that for our purpose allow calculation of $(\Delta V/V_{\text{sphere}})_{\max}$ for $N\geq 5$ (Table I).

For up to $N=4$, the necessary condition is not sufficient. This is obvious for $N=2$: the caps corresponding to the solutions of the Tammes' problem are two hemispheres ($\alpha=90°$), which cannot be simultaneously reverted. Interpenetration of two opposite depressions begins when they contact at the center of the sphere, which corresponds to a maximum value of the depression half-angle α: $\alpha_{\max,2}=60°$. We will repeat a likewise operation in what follows, by keeping the centers of the spherical caps of the Tammes' problem solutions at their positions, then decreasing α to a value for which there is no interpenetration. For $N=3$, the caps that solve the Tammes' problem are centered on the vertices of an equilateral equatorial triangle [24]; a little trigonometry shows that interpenetration is avoided when α reduces to $\alpha_{\max,3}$, with $\cos\alpha_{\max,3}=1/\sqrt{3}$ (Fig. 4). In a similar way, one can show for $N=4$ that $\cos\alpha_{\max,4}=1/(2\sin\alpha_T/2)$, where $\alpha_T=109°$ is the angle between two center/vertex directions in the tetrahedron. Hence, the half-angle of 54.59° (Tammes' problem solution for $N=4$, with tetrahedric symmetry) corresponds to 52.24° for the noninterpenetrating inverted caps. For higher values of N ($N>4$), the polyhedron holding the bases of the spherical caps present only right or obtuse angles between adjacent faces. There is therefore no risk of interpenetration as long as the cap bases do not overlap, and the Tammes' condition is sufficient.

With these values of $\alpha_{\max,N}$, the maximum relative volume variation $(\Delta V/V_{\text{sphere}})_{\max,N}$ can be calculated for each N (Table I). For all N, $\Delta V/V_{\text{sphere}}$ has no physical meaning above $(\Delta V/V_{\text{sphere}})_{\max,N}$ [as shown before, the mathematical solution provided by Eqs. (3a) and (3b) corresponds to interpenetration of the inverted caps beyond this limit]; hence, the energy U_N of the state with N depressions is plotted and considered only up to $(\Delta V/V_{\text{sphere}})_{\max,N}$ in Fig. 3. We also restrict to values of N from 1 to 6, because higher values correspond to energies superior to U_6 for physical values of $\Delta V/V_{\text{sphere}}$ [i.e., smaller than $(\Delta V/V_{\text{sphere}})_{\max,N}$].

Looking for the number N of depressions that correspond to the lowest energy at every relative volume variation provides the phase diagram displayed in Fig. 5. At first, the optimum N increases with $\Delta V/V_{\text{sphere}}$ due to energetic considerations, from $N=1$ up to a quite stable cubic organization of the depressions ($N=6$). The cap half-angle α keeps a value of around 40° during this evolution. Then steric factors favor a tetrahedric-related conformation ($N=4$), followed by the final single depression state. It is interesting to note that the state $N=1$ for high relative volume variations is made compulsory by the geometry: this explains *a posteriori* why there is no point in refining the energy calculation in this limit.

In observations by Gao *et al.* [8], which correspond obviously to a zero spontaneous curvature case as the capsule is composed of symmetrical polyelectrolyte layers, single depressions were observed for angles up to 46° for osmotic pressures of 22 kPa, and beyond 76° for 44.5 kPa (increase of osmotic pressure leads to a loss of inner volume), as displayed in Fig. 1(b). This is not far from the upper and lower limits for $N=1$, which suggests that it could be worthwhile exploring intermediate values of the osmotic pressure in order to check the presence of configurations presenting a higher number of depressions. In a similar but thinner system ($d/R=0.018$), a transition from $N=1$ toward a higher number of depressions was observed when increasing the osmotic pressure [25], but a further increase leads to a zoology of tortured shapes for which we do not have a model. With localized occurrence of important curvature, coalescence of

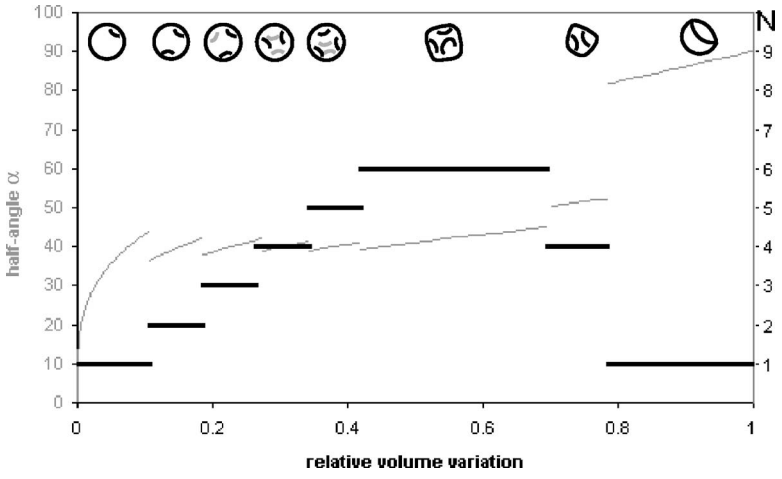

FIG. 5. Black (right axis): Equilibrium values of the number of similar depressions N at the surface of the , as a function of the relative volume variation $\Delta V/V$. The five first transitions occur at $\Delta V/V_{\text{sphere}}=0.106$, 0.185, 0.274, 0.341, and 0.418. The following "steric" transitions occur at values given in Table I for $N=6$ and $N=4$. Gray (left axis): In degrees, half-angle α of the depressions.

distinct depressions can be prevented by high energy barriers. This would lead to quenching of the system in metastable conformations, which is not rare in buckling problems.

In the present model of zero spontaneous curvature, a single parameter (the total relative volume variation) happens to drive the conformations; this is worthwhile to note. As previously stated, we did not consider the extension of the circular ridge that continuously links the inverted cap to the spherical undeformed part. Taking it into account would (i) increase for each depression the volume variation by a term scaling in $\delta^2 R$, which means a correction in $N(d/R)$ for $\Delta V/V_{\text{sphere}}$; (ii) lower the maximum surface compactness of depressions by adding an excluded corona around the caps (of width or order δ), which amounts to decrease $d_{\max,N}$ and then $(\Delta V/V_{\text{sphere}})_{\max,N}$ for each N. If the prefactor of d/R in the volume correction varies slowly with α, the global effect of (i) will be a displacement of the transitions toward smaller values of $\Delta V/V_{\text{sphere}}$, proportionally to d/R. Besides, by affecting $(\Delta V/V_{\text{sphere}})_{\max,N}$, (ii) will cause an additional displacement of the "steric" transitions (i.e., transitions toward smaller values of N). Another consequence is a concomitant lowering of the range of α for the corresponding conformations, decreasing in particular the minimum value of α that can be obtained for the capsule. Both effects vanish for the thinnest shells, which is likely to be the case in aforementioned references.

III. SHELLS OF NONZERO SPONTANEOUS CURVATURE

In this section, the reference state of the shell surface has a spontaneous (algebric) curvature c_0 (surface being oriented toward the outside: for example, an initially unstrained case corresponds to $c_0=+1/R$). Curvature energy per unit surface then becomes $\kappa(c-c_0)^2/2$ instead of $\kappa c^2/2$, where c is the local mean curvature. The elastic energy of the ridge [19] can then be expressed as $U_{\text{ridge}}=2\pi\kappa\delta R \sin\alpha[(\delta/\tan\alpha)^{-1}-c_0]^2$.

In the region enclosed by the ridge, changing the curvature of a spherical cap of surface $2\pi R^2(1-\cos\alpha)$ from $(+1/R)$ to $(-1/R)$ costs an energy $U_{\text{cap}}=2\pi\kappa R^2(1-\cos\alpha)4c_0/R$. The total elastic energy of a single depression is then written

$$U_{1,\lambda}=2\pi\kappa(d/R)^{-1/2}[\sin\alpha(\tan\alpha-\lambda)^2+4(1-\cos\alpha)\lambda] \tag{5}$$

where $\lambda=c_0R(d/R)^{1/2}$. Equation (5) shows that the relative volume variation is not the only parameter anymore that drives the conformations. The relative thickness d/R and the relative spontaneous curvature c_0R also play a qualitatively similar role.

For various values of λ, we used this $U_{1,\lambda}$ like U_1 in Sec. II, in order to trace $U_{N,\lambda}$ as a function of $\Delta V/V_{\text{sphere}}$ for different numbers of depressions N, and then to determine which N has the lowest energy. Results are summarized in Fig. 6, that displays the phase diagram of the optimal N according to λ and $\Delta V/V_{\text{sphere}}$. In particular, the angle of a small single depression (corresponding to the upper limit of the $N=1$ region for low relative volume variations) varies from 44° for $\lambda=0$ to 60° for $\lambda=-1.2$ and to 66° for $\lambda=1.2$.

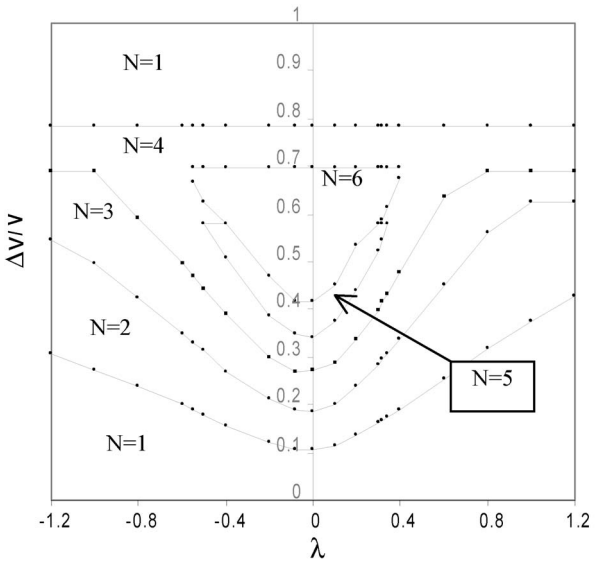

FIG. 6. Phase diagram displaying the equilibrium value of N (number of similar depressions) for shells of nonzero spontaneous curvature c_0. Vertical axis: Relative volume variation $\Delta V/V_{\text{sphere}}$. Horizontal axis: Adimensional curvature parameter $\lambda=c_0R(d/R)^{1/2}$.

For comparison with experimental results, we can remark that due to *in situ* formation, the elastic shell composed of aggregated polystyrene colloids of Ref. [7] should be unstrained; hence, $c_0R=1$ and $\lambda=(d/R)^{1/2}=0.3$ in this case. The phase diagram shows that one can find a range of $\Delta V/V_{\text{sphere}}$ presenting a $N=6$ state for this value.

For what concerns the *capsules* of [6,26], it is hard to propose an *a priori* value for λ. The templated spherical shells these capsules were obtained from must have been strainless after their synthesis, but subsequent modification of inner and outer solvent is likely to have caused a nonzero spontaneous curvature due to asymmetric surface charge. Interestingly enough, the steric boundaries of the phase diagram are not affected by λ; hence, the observation of capsules with a single depression of half-angle ~90° is consistent with the position of the upper $N=1$ zone, whatever the value of λ.

IV. CONCLUSION

We showed that a relatively simple model of elastic deformations at equilibrium, and mainly by curvature, is sufficient to make the first predictions concerning postbuckling conformations of a spherical shell submitted to an external pressure. In this model, the parameters that drive the transitions between different states (i.e., different number of depressions formed by inversion of a spherical cap) are the total relative volume variation and the adimensional curvature parameter λ, taking into account both the thickness of the shell and its spontaneous curvature (rescaled by the initial sphere radius). The buckled sphere exhibits a single depression for both small and important relative volume variations, and several depressions (up to six, which leads to a cubic symmetry) for intermediate ones. This model proposes a phase diagram that is likely to explain the conformations

observed in experiments: "capsules" with a nearly hemispheric single depression for important variations of the inner volume, observed by Zoldesi *et al.* [6,26], other $N=1$ states observed by Gao *et al.* [8], or coarsely cubic shapes for weaker variations observed by Tsapis *et al.* [7]. For more accurate predictions, a more sophisticated model considering the geometry of the ridge is required. It should reveal, at higher orders, an extra influence of the relative shell thickness d/R on the boundaries of the phase diagram.

ACKNOWLEDGMENTS

The author thanks E. B. Saff, R. Ferreol, and J.-P. Raven for interesting suggestions, F. Graner and J.-P.R. for careful reading of the manuscript, and B. Houchmandzadeh for his introduction to Scilab. Financial support was granted from D.G.A. (Direction Générale de l'Armement) and the Transregio Template Program.

[1] S. Kitipornchai, W. J. Kang, H. F. Lam, *et al.*, J. Constr. Steel Res. **61**, 764 (2005), and references herein.
[2] S. Sabouri-Ghomi, M. H. K. Kharrazi, and P. Javidan, Thin-Walled Struct. **44**, 152 (2006).
[3] G. Portela and L. A. Godoy, J. Constr. Steel Res. **61**, 808 (2005).
[4] Good review of recent advances in S. Komura, K. Tamura, and T. Kato, Eur. Phys. J. E **18**, 343 (2005).
[5] M. Stein, AIAA J. **6**, 2339 (1968); reedited in J. Spacecr. Rockets **40**, 908 (2003).
[6] C. I. Zoldesi and A. Imhof, Adv. Mater. (Weinheim, Ger.) **17**, 924 (2005).
[7] N. Tsapis, E. R. Dufresne, S. S. Sinha *et al.*, Phys. Rev. Lett. **94**, 018302 (2005).
[8] C. Gao, E. Donath, S. Moya *et al.*, Eur. Phys. J. E **5**, 21 (2001).
[9] L. Landau and E. M. Lifshitz, *Theory of Elasticity*, 3rd ed. (Elsevier Butterworth-Heinemann, Oxford, 1986), and textbooks. Reference [4] also writes down very clearly these calculations.
[10] A. V. Pogorelov, *Bendings of Surfaces and Stability of Shells* (American Mathematical Society, Providence, 1988).
[11] W. Wunderlich and U. Albertin, Int. J. Non-Linear Mech. **37**, 589 (2002).
[12] W. Helfrich, Z. Naturforsch [C] **28C**, 693 (1973).
[13] L. Miao, U. Seifert, M. Wortis, and , H.-G. Döbereiner,Phys. Rev. E **49**, 5389 (1994).
[14] R. Mukhopadhyay, G. H. W. Lim, and M. Wortis, Biophys. J. **82**, 1756 (2002).
[15] Among many papers dealing with this subject: R. Lipowsky, Nature (London) **349**, 475 (1991).
[16] G. H. W. Lim, M. Wortis, and R. Mukhopadhyay, Proc. Natl. Acad. Sci. U.S.A. **99**, 16766 (2002).
[17] J. Lidmar, L. Mirny, and D. R. Nelson, Phys. Rev. E **68**, 051910 (2003).
[18] L. Pauchard and Y. Couder, Europhys. Lett. **66**, 667 (2004).
[19] L. Pauchard, Y. Pomeau, and S. Rica, C. R. Acad. Sci., Ser. IIb: Mec., Phys., Chim., Astron. **324**, 411 (1997).
[20] P. N. L. Tammes, Rec. Trav. Bot. Neerl. **27**, 1 (1930).
[21] J. H. Conway and N. J. A. Sloane, *Sphere Packing, Lattices and Groups* (Springer, New York, 1999).
[22] K. Schütte and B. L. van der Waerden, Math. Ann. **123**, 96 (1951).
[23] D. A. Kottwitz, Acta Crystallogr., Sect. A: Found. Crystallogr. **47**, 158 (1991).
[24] This can easily be understood, as the intersection between the plane defined by the three points and the sphere is a circle. Three points on a circle maximize their mutual separation with an equilateral spreading, and the point-to-point distance increases with the circle size, which is maximum when the circle is equatorial.
[25] C. Gao, S. Leporatti, S. Moya, E. Donath, and H. Möhwald, Langmuir **17**, 3491 (2001).
[26] C. I. Zoldesi, C. A. van Walree, and A. Imhof, Langmuir **22**, 4343 (2006).
[27] Y. Teshima and T. Ogawa, Forma **15**, 347 (2000).
[28] E. B. Saff and A. B. J. Kuijlaars, Math. Intell. **19**, 5 (1997).